AFRL-OSR-VA-TR-2014-0164

Polymer-based and polymer-templated nanostructured thermoelectric Devices

Anish Tuteja
UNIVERSITY OF MICHIGAN

07/23/2014
Final Report

Air Force Research Laboratory
AF Office Of Scientific Research (AFOSR)/ RTD
Arlington, Virginia 22203
Air Force Materiel Command

Report Documentation Page

Form Approved
OMB No. 0704-0188

1. REPORT DATE	2. REPORT TYPE	3. DATES COVERED
14 JUL 2014		**15-04-2011 to 15-04-2014**

4. TITLE AND SUBTITLE	5a. CONTRACT NUMBER
Polymer-based and Polymer-templated Nanostructured Thermoelectric Devices	5b. GRANT NUMBER
	5c. PROGRAM ELEMENT NUMBER
6. AUTHOR(S)	5d. PROJECT NUMBER
	5e. TASK NUMBER
	5f. WORK UNIT NUMBER
7. PERFORMING ORGANIZATION NAME(S) AND ADDRESS(ES) **University of Michigan,Division of Research Development and Administration,,503 Thompson St,,Ann Arbor,MI,48109**	8. PERFORMING ORGANIZATION REPORT NUMBER
9. SPONSORING/MONITORING AGENCY NAME(S) AND ADDRESS(ES)	10. SPONSOR/MONITOR'S ACRONYM(S)
	11. SPONSOR/MONITOR'S REPORT NUMBER(S)

12. DISTRIBUTION/AVAILABILITY STATEMENT
Approved for public release; distribution unlimited

13. SUPPLEMENTARY NOTES

14. ABSTRACT

15. SUBJECT TERMS

16. SECURITY CLASSIFICATION OF:			17. LIMITATION OF ABSTRACT	18. NUMBER OF PAGES	19a. NAME OF RESPONSIBLE PERSON
a. REPORT	b. ABSTRACT	c. THIS PAGE			
unclassified	**unclassified**	**unclassified**	**Same as Report (SAR)**	**24**	

Final Project Report: Polymer-based and Polymer-templated Nanostructured Thermoelectric Devices

Grant Number: FA9550-11-1-0017

PI: Dr. Anish Tuteja
Department of Materials Science and Engineering,
University of Michigan

Date: July 13, 2014.

Submitted to Dr. Charles Y-C. Lee,
Air Force Office of Scientific Research (AFOSR)
Email: charles.lee@afosr.af.mil

Executive Summary: This Young Investigator Proposal has so far lead to 10 publications in high impact journals, as well as, widespread domestic and international popular press coverage. Results from this work have also been presented in 15 different invited talks. The project involved five undergraduate students, two graduate students and a postdoctoral research associate. A few of the publications resulting from this work have been summarized below. A list of all 10 manuscripts published based on this work is provided in the end. Three more publications based on this work are either submitted or in preparation.

Manuscript 1: "Hierarchically structured superoleophobic surfaces with ultra-low contact angle hysteresis", Arun K. Kota, Yongxin Li, Joseph M. Mabry, and Anish Tuteja, ***Advanced Materials***, 2012, Volume 24, Issue 43, pages 5838–5843**.**
Journal Impact Factor: 14.829 **Times Cited:** 30

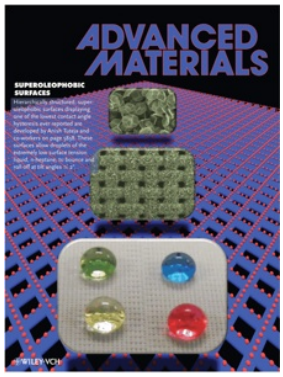

Summary: Superoleophobic surfaces can repel essentially any contacting liquid, including various low surface tension liquids. A surface is considered superoleophobic if the apparent contact angle θ^* for the contacting liquid droplet is greater than 150° and the surface displays low contact angle hysteresis $\Delta\theta^*$ (the difference between the advancing and receding contact angles).[1] While there are several natural and engineered superhydrophobic surfaces ($\theta^* > 150°$ and $\Delta\theta^* < 5°$ for water), there are no naturally occurring superoleophobic surfaces. This is because low surface tension liquids, such as various oils and alcohols, tend to easily wet and spread on most solid surfaces. Superhydrophobic surfaces have been extensively investigated, both experimentally and theoretically, in the past decade.[2-13] In comparison, there are significantly fewer publications on developing superoleophobic surfaces. In recent work, we[1,14-17] and others[18-20] explained how *re-entrant surface curvature* in conjunction with surface chemistry and roughness can be used to design

superoleophobic surfaces. While several surfaces have now been engineered with $\theta^* > 150°$ for various low surface tension liquids, none of them,[19-30] including our previous work,[1,14-17] reported a contact angle hysteresis $\Delta\theta^* < 5°$ with liquids possessing a surface tension lower than that of *n*-hexadecane (γ_{lv}= 27.5 mN m^{-1}). Note that $\Delta\theta^* < 5°$ has been reported before on surfaces that show low apparent contact angles ($\theta^* < 120°$).[31] However, such surfaces require a lubricating liquid film. Developing superoleophobic surfaces with ultra-low contact angle hysteresis can extend the applications of superhydrophobic surfaces to low surface tension liquids, as well as, open avenues to new applications. Such surfaces are expected to be critical for a range of applications including stain-free textiles and spill-resistant protective wear,[24] enhanced solvent-resistance,[29] self-cleaning,[9] reduction of bio-fouling,[32] finger-print resistant surfaces for flat-panel displays, cell-phones and sunglasses,[33] drag reduction,[34] developing truly 'non-stick' coatings and icephobicity.[35]

In this work, we developed a simple, single-step technique, based on electrospinning microbeads onto textured surfaces, to develop re-entrant, hierarchically structured, superoleophobic surfaces. We also demonstrated that we could tune the contact angle hysteresis on these hierarchical surfaces by systematically varying the inter-feature spacing for both the coarser length scale and the finer length scale features. The low surface energy and the significantly reduced solid-liquid contact area allow our hierarchically structured surfaces to exhibit ultra-low contact angle hysteresis even for extremely low surface tension liquids such as *n*-heptane (with $\theta_{oil} < 90°$). This ultra-low contact angle hysteresis allows, for the first time, droplets of essentially any contacting liquid, including *n*-heptane, to easily roll-off (roll-off angles $\omega \leq 2°$) and bounce on our surfaces. This result was particularly interesting given that the materials used to fabricate the superoleophobic surfaces are inherently *oleophilic*.

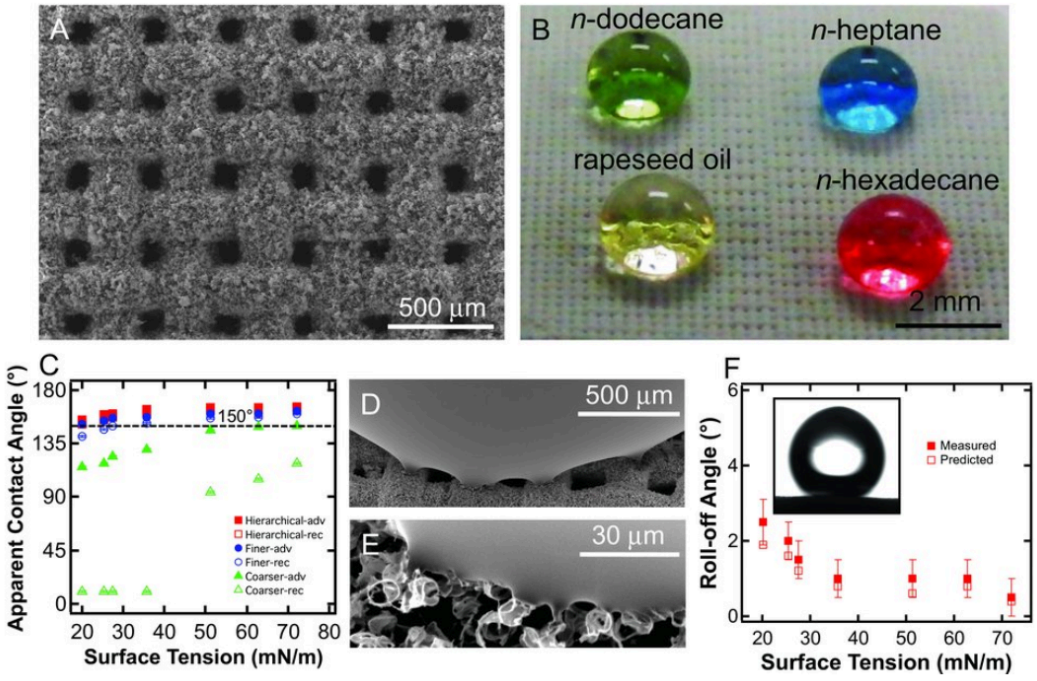

Figure 1. a) SEM image of a stainless steel mesh 70 uniformly coated with electrospun microbeads of 50 wt% fluorodecyl POSS + PMMA blend. B) Droplets of rapeseed oil (γ_{lv} = 35.7 mN m^{-1}), *n*-hexadecane (γ_{lv} = 27.5 mN m^{-1}), *n*-dodecane (γ_{lv} = 25.3 mN m^{-1}) and *n*-heptane (γ_{lv} = 20.1 mN m^{-1}) showing very high apparent contact angles on the surface shown in a). c) Advancing and receding apparent contact angles for various liquids on a hierarchically structured surface, as well as, on surfaces with the coarser length scale texture only and on surfaces with the finer length scale texture only. The receding contact angle legends are not visible for the hierarchically structured surfaces because of the ultra-low contact angle hysteresis. D) and e) SEM images showing the vicinity of the contact line along the coarser length scale texture and the finer length scale texture, respectively, of the hierarchically structured surface. The distortions in the contact line are evidence of air trapped at both the length scales. F) Roll-off angles of various liquids on the hierarchically structured surface. The inset shows a *n*-heptane droplet rolling on a hierarchical surface at a roll-off angle $\omega = 3°$.

Manuscript 2: "Patterned Superomniphobic-Superomniphilic Surfaces: Templates for Site-Selective Self-Assembly", Sai P.R. Kobaku, Arun K. Kota, Duck Hyun Lee, Joseph M. Mabry, and Anish Tuteja, ***Angewandte Chemie - International Edition***, 2012, 51, 10109.

Journal Impact Factor: 13.734 **Times Cited:** 13

Summary: Superhydrophobic surfaces display apparent contact angles greater than 150° and low contact angle hysteresis with water, while superoleophobic surfaces display apparent contact

angles greater than 150° and low contact angle hysteresis with low surface tension liquids such as oils and alcohols.[1,15-17] Superomniphobic surfaces display both superhydrophobicity and superoleophobicity. Similarly, superomniphilic surfaces display both superhydrophilicity and superoleophilicity i.e., apparent contact angles ~ 0° with both water and low surface tension liquids.[36] Patterned surfaces containing well defined domains that display both these extreme wetting properties have many potential applications in fog harvesting and liquid transport,[37,38] microchannels and microreactors,[39-44] enhanced condensation[45-47] and boiling[48-50] heat transfer, and the directed growth of thin films.[51-53] Further, such surfaces can also serve as templates for the wettability-driven self-assembly of liquids,[39-44] micro- or nano-particles,[54-57] and DNA.[58] However, the majority of patterned surfaces developed thus far exhibit extreme wettability contrast only with high surface tension liquids such as water (surface tension, γ_{lv} = 72.1 mN m^{-1}), thereby limiting the applications of such surfaces mostly to surfactant-free aqueous systems.[39-58]

In order to expand the application range to non-aqueous systems, especially those with low surface tension liquids such as oils (e.g., heptane, γ_{lv} = 20.1 mN m^{-1}) and alcohols (e.g., methanol, γ_{lv} = 22.5 mN m^{-1}), it is crucial to develop patterned superomniphobic-superomniphilic surfaces. While there have been a few reports on switchable superoleophobic-superoleophilic surfaces,[14,59-61] there are currently no reports on either superoleophobic or superomniphobic surfaces that are patterned with regular, well-defined superomniphilic domains (or vice-versa). Recent work[1,15-20] has explained how re-entrant surface texture, in conjunction with surface chemistry and roughness, can be used to design superomniphobic surfaces. In this work, we report a simple, fast and practical methodology to develop patterned superomniphobic-superomniphilic surfaces that exhibit stark contrast in wettability with a wide range of polar and non-polar liquids. Using these surfaces, we demonstrate the site-selective self assembly of

heptane upon dipping and spraying on textured surfaces, site-selective condensation and boiling with low surface tension liquids, and site-selective self-assembly of both polymers and microparticles.

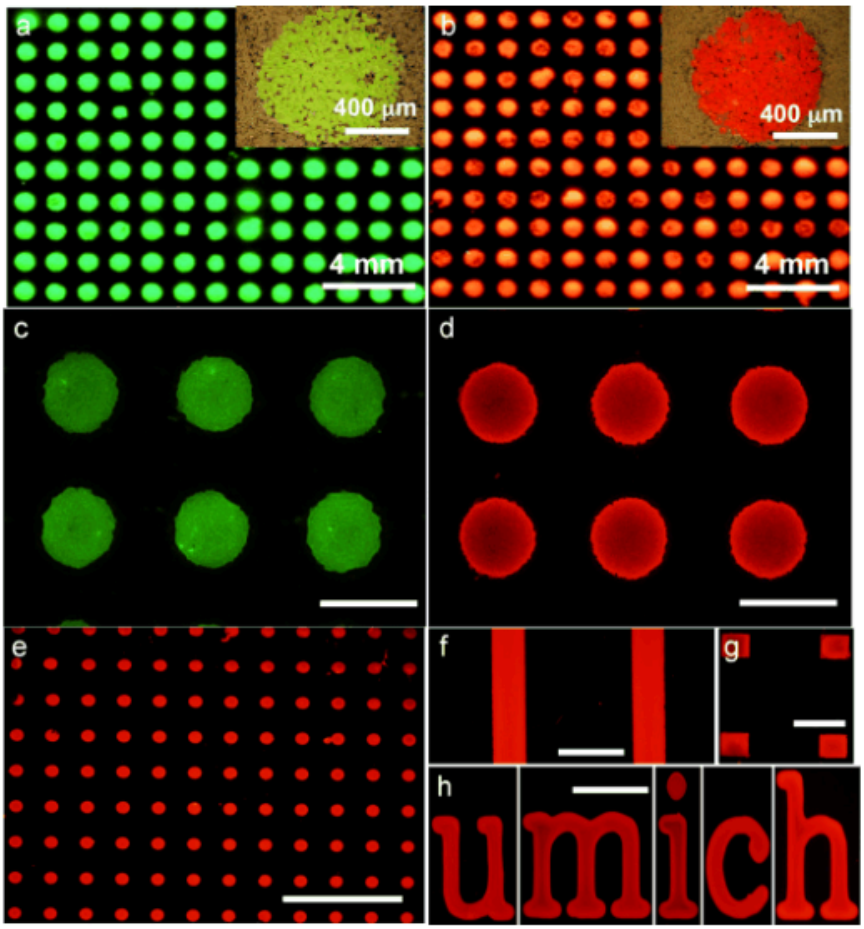

Figure 2: a) and b) Site-selective self-assembly of UV fluorescent green microspheres dispersed in water and UV fluorescent red microspheres dispersed in heptane, respectively. (a) and (b) were obtained under a 365 nm UV lamp and the corresponding insets show higher magnification optical microscope images. C) Site-selective self-assembly of PVP dissolved in water using 800 μm diameter circular superomniphilic domains. D) and e) Site-selective self-assembly of PIB dissolved in heptane using 800 μm and 100 μm diameter circular superomniphilic domains, respectively. F), g), and h) Site-selective self-assembly of PIB using superomniphilic domains of non-circular shapes. C), d), e), f), g) and h) were obtained using fluorescent microscopy and scale bars represent 1 mm.

Manuscript 3: "High Efficiency Thin Upgraded Metallurgical-Grade Silicon Solar Cells on Flexible Substrates", Jae Young Kwon, Duck Hyun Lee, Michelle Chitambar, Stephen Maldonado, Anish Tuteja, and Akram Boukai, ***Nano Letters***, 2012, 12, 10, 5143-5147.

Journal Impact Factor: 13.025 **Times Cited:** 9

Summary: The solar cell market has experienced tremendous growth in past several years, and silicon accounts for more than ~90 % of the market due to advantages of earth abundance, good reliability, performance and a wealth of silicon materials processing knowledge.[62-64] However, the high cost (> $1/W) of solar-grade Si solar cells has hindered their immediate adoption in the commercial market.[65-67] Currently, two major approaches have been pursued to reduce the cost of Si-based solar cells per watt: the adoption of low-cost Si such as metallurgical-grade (MG)[65,67] or upgraded MG (UMG) Si[68,69] and reducing the usage of Si material by preparing ultrathin solar modules.[70-72] UMG-Si is generally prepared by the chemical refining of raw Si,[73] and it costs ~$10 per kg, which makes it almost *5 – 10 times less expensive* than solar-grade Si.[74] The main disadvantage of UMG-Si is the high impurity level of the starting material leading to decreased minority-carrier lifetimes and device efficiency.[66,67] Solar cell modules composed of ultrathin microcells allow for increased efficiency with shorter collection pathways to the p-n junction, and also decrease the usage of Si. However, the efficiency of ultrathin microcells decreases steeply due to inadequate optical absorption.[70,71]

Nanoparticle and nanopillars arrays[75-79] are two structures that have been utilized for enhancing optical absorption in Si solar cells. Nanoparticles arrays on top of a semiconducting surface can enhance optical absorption through localized surface plasmon resonances (LSPR). LSPR[71,80-83] is the collective oscillation of conduction electrons stimulated by incident light at the interface between a metal (Ag, Au, Pt) and a dielectric, which enables the light to be concentrated and absorbed into the Si layer.[81] Both the silver nanoparticles and the nanopillars arrays formed on the Si surface can also significantly increase light absorption by one or more of the following three mechanisms: 1) scattering incident light at oblique angles thereby increasing

the optical path-length,[76] 2) substrate-coupled Mie resonances,[77] and 3) impedance matching caused by a tapered refractive index.[78] In this work, we have combined the absorption enhancement effects of both the nanoparticle and nanopillars arrays, by creating a periodic and uniform metal nanoparticle array on top of a hexagonally close-packed array of silicon nanopillars.[84] Various nanopatterning methods such as electron beam lithography[85] and nanoimprint lithography[86] have been previously employed to create periodic and uniform plasmonic metal nanoparticles. However, the low throughput of e-beam lithography due to serial processing, as well as, the difficulty in reproducing sub–50 nm features have severely limited their applicability.[85-87] An alternative emerging approach to prepare a nanopatterned periodic and uniform array of metal particles is through the use of block copolymer lithography.[82,88-91] Here we have developed thin film (< 20 μm) solar cells based on upgraded metallurgical-grade polycrystalline Silicon that utilize silver nanoparticles atop silicon nanopillars created by block copolymer nanolithography to enhance light absorption and increase cell efficiency $\eta > 8$ %. In addition, the solar cells are flexible and semi-transparent so as to reduce balance of systems costs and open new applications for conformable solar cell arrays on a variety of surfaces. Detailed studies on the optical and electrical properties of the resulting solar cells suggest that both anti-reflective and light trapping mechanisms are key to the enhanced efficiency.

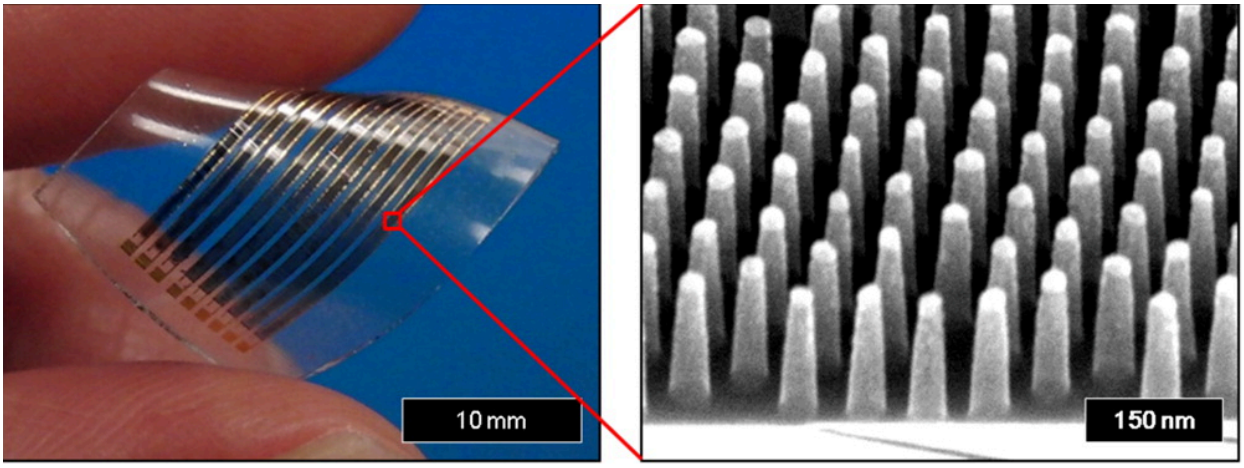

Figure 3: High Efficiency Thin Upgraded Metallurgical-Grade Silicon Solar Cells on Flexible Substrates

Manuscript 4: "Superomniphobic Surfaces for Effective Chemical Shielding", Shuaijun Pan, Arun K. Kota, Joseph M. Mabry and Anish Tuteja, ***Journal of the American Chemical Society*****,** 2013, 135 (2), 578–581

Journal Impact Factor: 10.677 **Times Cited:** 42

This work was highlighted by Univ. of Michigan, NBC News, Popular Science, Wall Street Journal, Chemistry World, The Daily Mail, ASME, NASA, Geek.com, Science Daily, American Bazaar, Slashdot, Canada Free Press, The Deccan Herald, and over 100 more domestic and international newspapers and websites.

Summary: Superhydrophobic surfaces display apparent contact angles $\theta^* > 150°$ and low contact angle hysteresis $\Delta\theta^*$ (the difference between the advancing and receding contact angles) with water, while superoleophobic surfaces display $\theta^* > 150°$ and low $\Delta\theta^*$ with low surface tension liquids.[1,15-17] Superomniphobic surfaces display both superhydrophobicity and superoleophobicity. While surfaces that display superomniphobicity with various Newtonian[92] liquids have been previously engineered,[19-30] there are few, if any, articles that report superomniphobicity with non-Newtonian[92] liquids. In this work, we report surfaces that display superomniphobicity with non-Newtonian liquids (e.g., viscoelastic polymer solutions) in addition to a wide range of Newtonian liquids including concentrated organic and inorganic acids, bases

and solvents. Virtually all liquids – organic or inorganic, polar or non-polar, Newtonian or non-Newtonian – easily roll-off and bounce on our surfaces, thereby making our surfaces ideal candidates for effective chemical shielding. We envision that our surfaces will have numerous applications including stain-free clothing and spill-resistant, breathable protective wear,[24] enhanced solvent-resistance,[29] bio-fouling resistant surfaces,[32] self-cleaning,[9] drag reduction,[34] and light-weight corrosion-resistant coatings.[93]

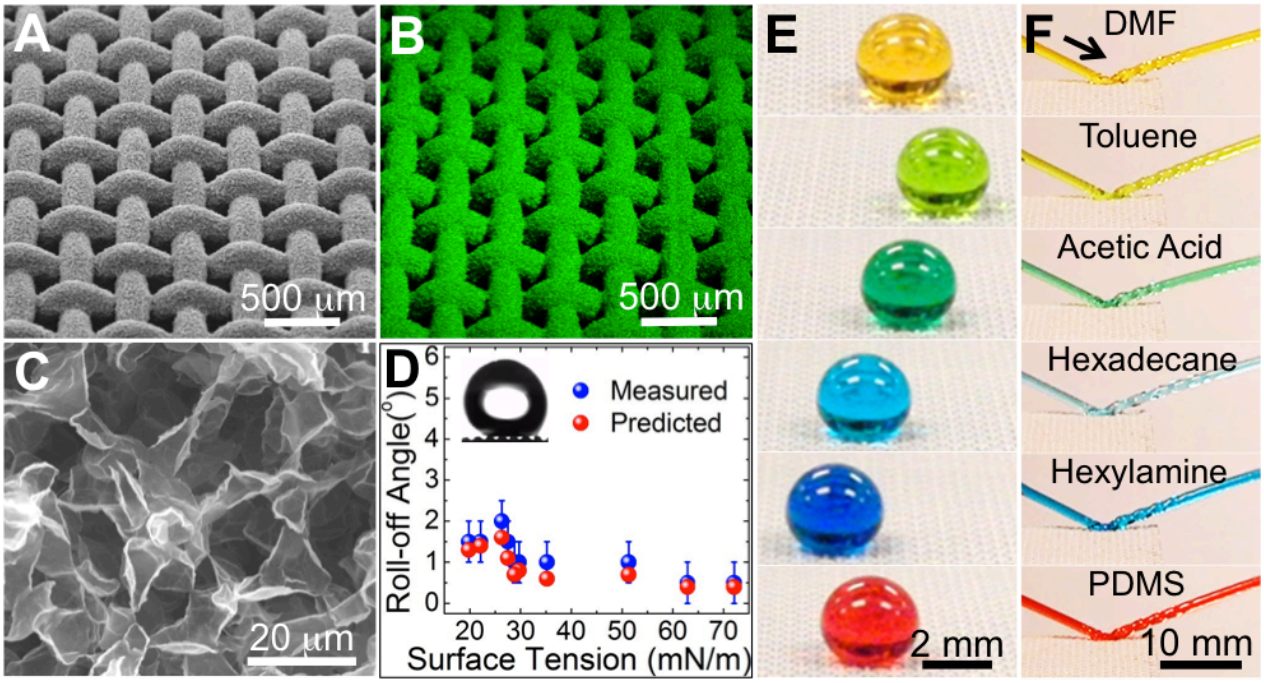

Figure 4. (a) An SEM image of the hierarchically structured surface illustrating the electrospun coating of cross-linked PDMS + 50 wt% fluorodecyl POSS on a stainless steel wire mesh 70. (b) Elemental mapping of fluorine on the hierarchically structured surface. The high surface fluorine content is expected to be due to the surface migration of the fluorodecyl POSS molecules. (c) An SEM image illustrating the re-entrant curvature of the electrospun texture. (d) Roll-off angles for various Newtonian liquids on the surface shown in (a). The inset shows an ethanol droplet rolling on the surface at a roll-off angle $\omega = 2°$. (e) Droplets of various low surface tension Newtonian liquids showing very high contact angles on the surface shown in (a). (f) Jets of different Newtonian liquids shown in (e) bouncing on the surface shown in (a).

Manuscript 5: "Transparent, Flexible, Superomniphobic Surfaces with Ultra-Low Contact Angle Hysteresis", ***Angewandte Chemie International Edition,*** Kevin Golovin, Duck Hyun Lee, Joseph M. Mabry, and **Anish Tuteja** [#], 2013, 52, 49, 13007–13011, December 2, 2013

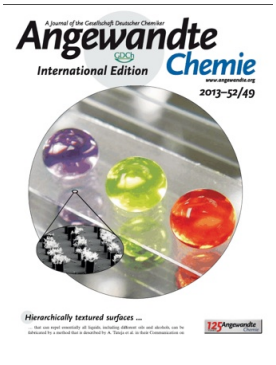

Journal Impact Factor: 13.734 **Times Cited:** 2

Summary: Engineered surfaces that repel low surface tension liquids such as various oils and alcohols have a wide array of applications including stain-proof apparel, fuel transport, chemical shielding and self-cleaning. Superomniphobic surfaces display apparent contact angles (θ^*) greater than 150° and exhibit low contact angle hysteresis (the difference between advancing and receding contact angles) with essentially all liquids. Previous work has shown how re-entrant curvature is necessary for repelling low surface tension liquids. However, it is typically difficult to obtain ultra-low contact angle hysteresis (CAH, $\Delta\theta^* < 5^o$) with such low surface tension liquids. In our recent work, we discussed the critical role of hierarchical texture in developing superomniphobic surfaces with ultra-low $\Delta\theta^*$. Unfortunately, such hierarchical, superomniphobic surfaces are usually opaque. The development of transparent superomniphobic surfaces is essential for a range of applications such as coatings for windows, phones, tablets, and computer screens. In this work we present a facile methodology for the development of flexible, highly transparent (optical transmission >90%), superomniphobic surfaces that can repel a range of low and high surface tension liquids.

At the time of writing, only a handful of transparent, omniphobic surfaces have been fabricated. None of these surfaces possesses hierarchical texture, which yields ultra-low values for $\Delta\theta^*$. In most previous studies, transparency was only achieved at the cost of lower θ^* and / or higher $\Delta\theta^*$ for low surface tension liquids. In this work, using previously developed design parameters, we are able to tune the texture of our surfaces to develop one of the first transparent superomniphobic surfaces with ultra-low contact angle hysteresis.

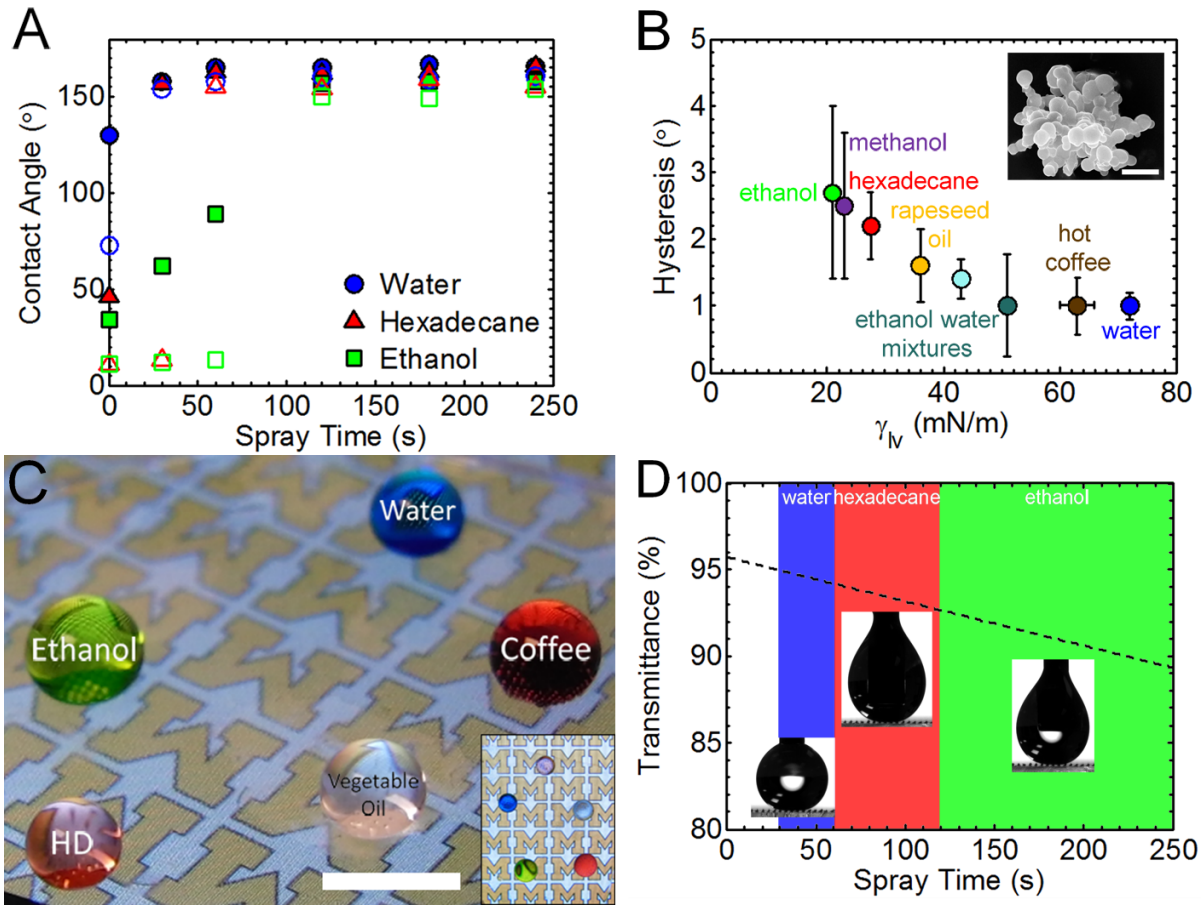

Figure 5. A-B) Contact angle measurements with water, hexadecane and ethanol for pillars with D*=100. Filled symbols are advancing angles, and the open symbols are receding contact angles. The surface in B) is sprayed for 120 seconds. The inset shows the reentrant PDMS+F-POSS structure; scale bar is 5 μm. C) Droplets of varying surface tension beading up on an Apple iPhone® 3GS screen coated with 20 μm pillars with D* = 42, and spray coated with PDMS+F-POSS for 120 seconds. The inset shows the top view of the same droplets to highlight the coating's transparency. The scale bar is 500 μm. D) A design diagram for D* = 100 pillars combining transparency and repellency characteristics. The insets are optical images of droplets (from left to right) of water, hexadecane and ethanol sitting atop the spray coated pillars. Note the composite interface is clearly visible underneath the liquid droplets.

Manuscript 6: "Extreme Light Absorption by Multiple Plasmonic Layers on Upgraded Metallurgical Grade Silicon Solar Cells", ***Nano Letters***, Duck Hyun Lee, Jae Young Kwon, Stephen Maldonado, Anish Tuteja, and Akram Boukai[#], 2014, 14 (4), 1961–1967.

Journal Impact Factor: 13.025 **Times Cited:** 0

Summary: Currently, silicon-based solar cells account for more than 90% of the solar cell market[62-64]. Most commercial, silicon-based solar cells utilize crystalline silicon wafers whose thickness varies between 180 – 300 μm. For the solar cell market to continue its rapid growth,

there must be significant progress in lowering the solar cell module costs and the balance of system costs[65-67]. These costs in turn are dominated by the costs of the silicon raw material[70,71,94], silicon purification[65,67-69], as well as, the installation of the completed solar cell module[70,94]. In this work we attempt to meet these challenges by i) reducing the amount of silicon material used by producing ultrathin ($t \sim 10$ μm) solar cells, ii) adopting relatively impure, low-cost substrates in the form of upgraded metallurgical-grade (UMG) silicon, and iii) developing flexible solar cells to lower installation costs.

The main challenge in developing solar cells utilizing thin silicon films is poor absorption[70,71]. Silicon has an indirect bandgap and thus requires the assistance of phonons for light absorption. This property hinders the efficient absorption of light and as a result requires the use of thick silicon ($t > 100$ μm). Therefore, improving the efficiency of an ultrathin, indirect bandgap solar cell requires engineering of the cell surface so that the light absorbance can be significantly increased.

Several methods have been investigated thus far to increase the light absorbance of thin solar cells, including dielectric anti-reflection coatings[95,96], surface texturing[75,76,78,97-99], and utilizing surface plasmon resonance[71,80,81,83]. Amongst these approaches, surface plasmon resonance is a particularly exciting methodology for achieving dramatically higher light absorption in ultrathin solar cells. A plasmon is the collective oscillation of conduction electrons stimulated by incident light at the interface between a metal (Ag, Au, Pt) and a dielectric. Both the shape and the size of the metal are key factors in determining the coupling between the metal particle and the dielectric, and thereby the overall enhancement in the optical absorption efficiency caused by surface plasmonic resonance[81]. Further, precise three-dimensional placement of plasmonic metal particles can also be used to effectively concentrate light on top of the solar cell, and thereby increase its conversion efficiency[100]. Indeed, it has been recently shown that metallic plasmonic nanoparticles can dramatically increase the short circuit current in silicon solar cells[81,94]. One methodology for enabling, high-throughput, large-scale assembly of

an array of plasmonic metallic nanoparticles on top of a solar cell is block copolymer nanolithography[82,90,101-104]. In this work, we fabricate multiple plasmonic layers (either double or quadruple plasmonic nanoparticle layers) on top of ultrathin UMG-silicon solar cells using block copolymer nanolithography. These plasmonic nanoparticle layers act as highly efficient light absorbing coatings that dramatically improve the optical absorption of the developed solar cells. This scalable approach increases the optical absorptivity for our solar cells to ~ 98% over a broad range of wavelengths, and they achieve efficiencies of ≈ 11%, which is a 300% increase over their bulk counterparts. The low-grade *and* ultra-thin silicon films used in the developed cells lower raw material costs, while the flexibility of the cells can lead to lower balance of systems costs. Detailed studies on the electrical and optical properties of the developed solar cells elucidate the light absorption contribution of each individual plasmonic layer. Finite-difference time-domain (FDTD) simulations were also performed to yield further insights into the obtained results. We anticipate that the findings from this work will provide useful design considerations for fabricating a range of different solar cell systems.

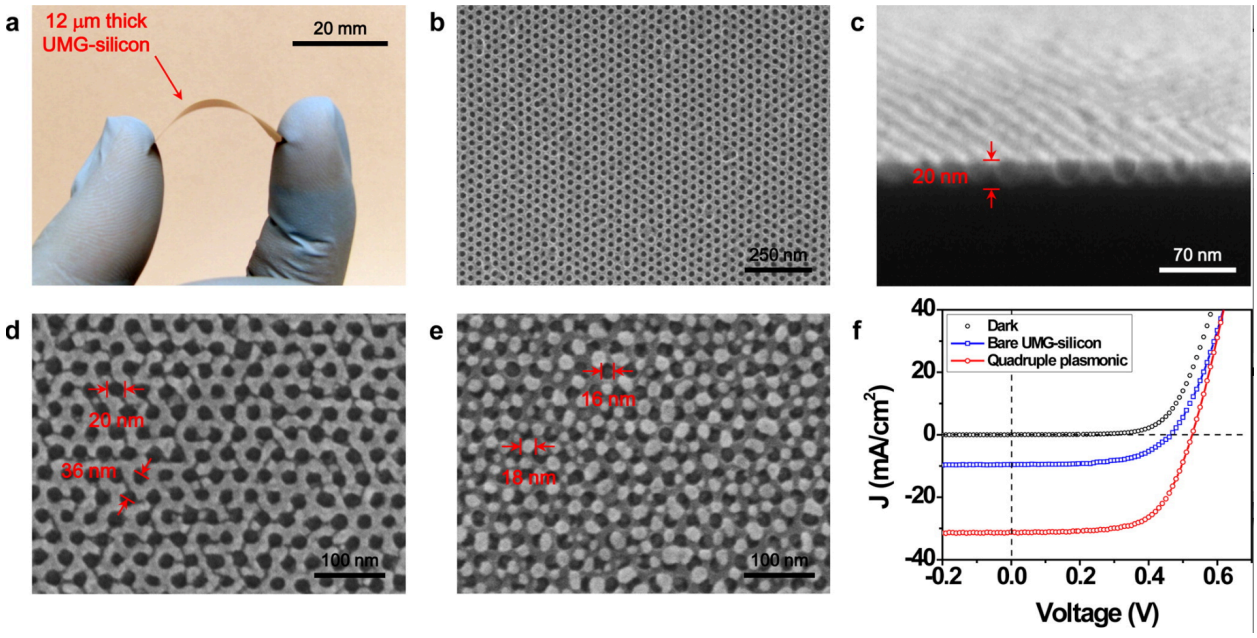

Figure 6. a, *J–V* curves for bare UMG-silicon (black), nanoporous UMG-silicon (blue), silver based double plasmonic layer on UMG-silicon (green), silver based double plasmonic layer (DPL) along with a top coating of spin on glass (green), UMG-silicon with a silver based quadruple plasmonic layer (red), and quadruple plasmonic layer without silver nanoparticles (Brown). Note the thickness of UMG-silicon is 180 μm. b, Absorbance spectrums for bare UMG-silicon (black), silver based double plasmonic layer on UMG-silicon (green) and silver based quadruple plasmonic layer on UMG-silicon (red). c, Quantum efficiency curves for bare UMG-silicon (black), quadruple plasmonic layer without silver nanoparticles (blue), silver based double plasmonic layer on UMG-silicon (green) and silver based quadruple plasmonic layer on UMG-silicon (red). d, V_{OC} and fill factors (*FF*) for each sample. e, f and g, Power absorption profiles calculated by finite difference time domain (FDTD) model under an incident light of 600 nm along the x-z plane of bare silicon (e), silver based double plasmonic layer on silicon (f) and silver based quadruple plasmonic layer on silicon (g). Note the incident light is propagating along the z-axis and is polarized along the *x*-axis. White dotted lines show surfaces of silicon (near 0 nm) and SiO_2 (near 100 nm).

A list of published manuscripts supported by this grant:

1. "The design and applications of superomniphobic surfaces", ***NPG Asia Materials,*** Arun K. Kota, Gibum Kwon and Anish Tuteja , 2014, 6, e109.
Journal Impact Factor: 9.042 Times Cited: 0

2. "Extreme Light Absorption by Multiple Plasmonic Layers on Upgraded Metallurgical Grade Silicon Solar Cells", ***Nano Letters***, Duck Hyun Lee, Jae Young Kwon, Stephen Maldonado, Anish Tuteja, and Akram Boukai, 2014, 14 (4), 1961–1967.
Journal Impact Factor: 13.025 Times Cited: 0

3. "Transparent, Flexible, Superomniphobic Surfaces with Ultra-Low Contact Angle Hysteresis", ***Angewandte Chemie International Edition,*** Kevin Golovin, Duck Hyun Lee, Joseph M. Mabry, and Anish Tuteja , 2013, 52, 49, 13007–13011, December 2, 2013 (**Highlighted as journal cover**)
Journal Impact Factor: 13.734 Times Cited: 2

4. "High-efficiency, ultrafast separation of emulsified oil–water mixtures", ***NPG Asia Materials***, Arun K. Kota and Anish Tuteja, 2013, 5, e58; doi:10.1038/am.2013.34
Journal Impact Factor: 9.042 Times Cited: 1

5. "Superomniphobic Surfaces: Design and Durability", ***MRS Bulletin***, Arun K. Kota, Wonjae Choi**,** and Anish Tuteja, 2013, 38, 5, 383-390.
Journal Impact Factor: 5.024 Times Cited: 12

6. "Superoleophobic surfaces: design criteria and recent studies", Arun K. Kota, Joseph M. Mabry, and Anish Tuteja, ***Surface Innovations,*** 2013, 1, 2, 71-83.
Journal Impact Factor: NA Times Cited: 1

This paper was awarded the "**best science paper award**" by the Institute of Civil Engineers.

7. "Superomniphobic Surfaces for Effective Chemical Shielding", Shuaijun Pan, Arun K. Kota, Joseph M. Mabry and Anish Tuteja, ***Journal of the American Chemical Society*****,** 2013, 135 (2), 578–581
Journal Impact Factor: 10.677 Times Cited: 42

This work was highlighted by Univ. of Michigan, NBC News, Popular Science, Wall Street Journal, Chemistry World, The Daily Mail, ASME, NASA, Geek.com, Science Daily, American Bazaar, Slashdot, Canada Free Press, The Deccan Herald, and over 100 more domestic and international newspapers and websites.

8. "High Efficiency Thin Upgraded Metallurgical-Grade Silicon Solar Cells on Flexible Substrates", Jae Young Kwon, Duck Hyun Lee, Michelle Chitambar, Stephen Maldonado, Anish Tuteja, and Akram Boukai, ***Nano Letters***, 2012, 12, 10, 5143-5147.
Journal Impact Factor: 13.025 Times Cited: 9

9. "Patterned Superomniphobic-Superomniphilic Surfaces: Templates for Site-Selective Self-Assembly", Sai P.R. Kobaku, Arun K. Kota, Duck Hyun Lee, Joseph M. Mabry, and Anish Tuteja, ***Angewandte Chemie - International Edition***, 2012, 51, 10109.
Journal Impact Factor: 13.734 Times Cited: 13

10. "Hierarchically structured superoleophobic surfaces with ultra-low contact angle hysteresis", Arun K. Kota, Yongxin Li, Joseph M. Mabry, and Anish Tuteja**,** ***Advanced Materials*****,** 2012, 24, 5838-5843. (**Highlighted as journal cover**)
Journal Impact Factor: 14.829 Times Cited: 30

References

1 Tuteja, A., Choi, W., Mabry, J. M., McKinley, G. H. & Cohen, R. E. Robust omniphobic surfaces. *Proceedings of the National Academy of Sciences of the United States of America* **105**, 18200-18205, doi:10.1073/pnas.0804872105 (2008).

2 Gao, L. C. & McCarthy, T. J. The "lotus effect" explained: Two reasons why two length scales of topography are important. *Langmuir* **22**, 2966-2967, doi:10.1021/la0532149 (2006).

3 Genzer, J. & Efimenko, K. Creating long-lived superhydrophobic polymer surfaces through mechanically assembled monolayers. *Science* **290**, 2130-2133, doi:10.1126/science.290.5499.2130 (2000).

4 Lafuma, A. & Quere, D. Superhydrophobic states. *Nature Materials* **2**, 457-460, doi:10.1038/nmat924 (2003).

5 Marmur, A. The lotus effect: Superhydrophobicity and metastability. *Langmuir* **20**, 3517-3519, doi:10.1021/la036369u (2004).

6 Ming, W., Wu, D., van Benthem, R. & de With, G. Superhydrophobic films from raspberry-like particles. *Nano Letters* **5**, 2298-2301, doi:10.1021/nl0517363 (2005).

7 Patankar, N. A. On the modeling of hydrophobic contact angles on rough surfaces. *Langmuir* **19**, 1249-1253, doi:10.1021/la026612+ (2003).

8 Quere, D. Non-sticking drops. *Reports on Progress in Physics* **68**, 2495-2532, doi:10.1088/0034-4885/68/11/r01 (2005).

9 Sun, T. L., Feng, L., Gao, X. F. & Jiang, L. Bioinspired surfaces with special wettability. *Accounts of Chemical Research* **38**, 644-652, doi:10.1021/ar040224c (2005).

10 Bhushan, B. & Jung, Y. C. Natural and biomimetic artificial surfaces for superhydrophobicity, self-cleaning, low adhesion, and drag reduction. *Progress in Materials Science* **56**, 1-108, doi:10.1016/j.pmatsci.2010.04.003 (2011).

11 Herminghaus, S. Roughness-induced non-wetting. *Epl* **79**, doi:59901 10.1209/0295-5075/79/59901 (2007).

12 Li, W. & Amirfazli, A. A thermodynamic approach for determining the contact angle hysteresis for superhydrophobic surfaces. *J. Colloid Interface Sci.* **292**, 195-201, doi:10.1016/j.jeis.2005.05.062 (2005).

13 Li, W. & Amirfazli, A. Microtextured superhydrophobic surfaces: A thennodynarnic analysis. *Adv. Colloid Interface Sci.* **132**, 51-68, doi:10.1016/j.cis.2007.01.001 (2007).

14 Choi, W. *et al.* Fabrics with Tunable Oleophobicity. *Advanced Materials* **21**, 2190-2195, doi:10.1002/adma.200802502 (2009).

15 Tuteja, A. *et al.* Designing superoleophobic surfaces. *Science* **318**, 1618-1622, doi:10.1126/science.1148326 (2007).

16 Chhatre, S. S. *et al.* Scale Dependence of Omniphobic Mesh Surfaces. *Langmuir* **26**, 4027-4035, doi:10.1021/la903489r (2010).

17 Tuteja, A., Choi, W., McKinley, G. H., Cohen, R. E. & Rubner, M. F. Design parameters for superhydrophobicity and superoleophobicity. *Mrs Bulletin* **33**, 752-758, doi:10.1557/mrs2008.161 (2008).

18 Marmur, A. From hygrophilic to superhygrophobic: Theoretical conditions for making high-contact-angle surfaces from low-contact-angle materials. *Langmuir* **24**, 7573-7579, doi:10.1021/la800304r (2008).

19 Ahuja, A. *et al.* Nanonails: A simple geometrical approach to electrically tunable superlyophobic surfaces. *Langmuir* **24**, 9-14, doi:10.1021/la702327z (2008).

20 Cao, L., Price, T. P., Weiss, M. & Gao, D. Super water- and oil-repellent surfaces on intrinsically hydrophilic and oleophilic porous silicon films. *Langmuir* **24**, 1640-1643, doi:10.1021/la703401f (2008).

21 Tsujii, K., Yamamoto, T., Onda, T. & Shibuichi, S. Super oil-repellent surfaces. *Angewandte Chemie-International Edition in English* **36**, 1011-1012, doi:10.1002/anie.199710111 (1997).

22 Li, H. J. *et al.* Super-"amphiphobic" aligned carbon nanotube films. *Angew. Chem.-Int. Edit.* **40**, 1743-1746, doi:10.1002/1521-3773(20010504)40:9<1743::aid-anie17430>3.0.co;2-# (2001).

23 Hsieh, C. T., Wu, F. L. & Chen, W. Y. Contact Angle Hysteresis and Work of Adhesion of Oil Droplets on Nanosphere Stacking Layers. *Journal of Physical Chemistry C* **113**, 13683-13688, doi:10.1021/jp9036952 (2009).

24 Leng, B. X., Shao, Z. Z., de With, G. & Ming, W. H. Superoleophobic Cotton Textiles. *Langmuir* **25**, 2456-2460, doi:10.1021/la8031144 (2009).

25 Steele, A., Bayer, I. & Loth, E. Inherently Superoleophobic Nanocomposite Coatings by Spray Atomization. *Nano Letters* **9**, 501-505, doi:10.1021/nl8037272 (2009).

26 Wang, D. A., Wang, X. L., Liu, X. J. E. & Zhou, F. Engineering a Titanium Surface with Controllable Oleophobicity and Switchable Oil Adhesion. *Journal of Physical Chemistry C* **114**, 9938-9944, doi:10.1021/jp1023185 (2010).

27 Fujii, T., Aoki, Y. & Habazaki, H. Fabrication of Super-Oil-Repellent Dual Pillar Surfaces with Optimized Pillar Intervals. *Langmuir* **27**, 11752-11756, doi:10.1021/la202487v (2011).

28 Darmanin, T. *et al.* Superoleophobic behavior of fluorinated conductive polymer films combining electropolymerization and lithography. *Soft Matter* **7**, 1053-1057, doi:10.1039/c0sm00837k (2011).

29 Zhang, J. P. & Seeger, S. Superoleophobic Coatings with Ultralow Sliding Angles Based on Silicone Nanofilaments. *Angew. Chem.-Int. Edit.* **50**, 6652-6656, doi:10.1002/anie.201101008 (2011).

30 Deng, X., Mammen, L., Butt, H.-J. r. & Vollmer, D. Candle Soot as a Template for a Transparent Robust Superamphiphobic Coating. *Science*, doi:10.1126/science.1207115 (2011).

31 Wong, T.-S. *et al.* Bioinspired self-repairing slippery surfaces with pressure-stable omniphobicity. *Nature* **477**, 443-447, doi:10.1038/nature10447 (2011).

32 Genzer, J. & Efimenko, K. Recent developments in superhydrophobic surfaces and their relevance to marine fouling: a review. *Biofouling* **22**, 339-360, doi:10.1080/08927010600980223 (2006).

33 Verho, T. *et al.* Mechanically Durable Superhydrophobic Surfaces. *Advanced Materials* **23**, 673-678, doi:10.1002/adma.201003129 (2011).

34 Lee, C. & Kim, C.-J. Underwater Restoration and Retention of Gases on Superhydrophobic Surfaces for Drag Reduction. *Physical Review Letters* **106**, doi:014502
10.1103/PhysRevLett.106.014502 (2011).

35 Ma, M. & Hill, R. M. Superhydrophobic surfaces. *Current Opinion in Colloid & Interface Science* **11**, 193-202, doi:10.1016/j.cocis.2006.06.002 (2006).

36 Koch, K., Blecher, I. C., Koenig, G., Kehraus, S. & Barthlott, W. The superhydrophilic and superoleophilic leaf surface of Ruellia devosiana (Acanthaceae): a biological model for spreading of water and oil on surfaces. *Functional Plant Biology* **36**, 339-350, doi:10.1071/fp08295 (2009).

37 Zhai, L. *et al.* Patterned superhydrophobic surfaces: Toward a synthetic mimic of the Namib Desert beetle. *Nano Letters* **6**, 1213-1217, doi:10.1021/nl060644q (2006).

38 Zheng, Y. *et al.* Directional water collection on wetted spider silk. *Nature* **463**, 640-643, doi:10.1038/nature08729 (2010).

39 Bruzewicz, D. A., Reches, M. & Whitesides, G. M. Low-cost printing of poly(dimethylsiloxane) barriers to define microchannels in paper. *Analytical Chemistry* **80**, 3387-3392, doi:10.1021/ac702605a (2008).

40 Carrilho, E., Martinez, A. W. & Whitesides, G. M. Understanding Wax Printing: A Simple Micropatterning Process for Paper-Based Microfluidics. *Analytical Chemistry* **81**, 7091-7095, doi:10.1021/ac901071p (2009).

41 Zahner, D., Abagat, J., Svec, F., Frechet, J. M. J. & Levkin, P. A. A Facile Approach to Superhydrophilic-Superhydrophobic Patterns in Porous Polymer Films. *Advanced Materials* **23**, 3030-+, doi:10.1002/adma.201101203 (2011).

42 Zhao, B., Moore, J. S. & Beebe, D. J. Surface-directed liquid flow inside microchannels. *Science* **291**, 1023-1026, doi:Doi 10.1126/Science.291.5506.1023 (2001).

43 Chitnis, G., Ding, Z., Chang, C.-L., Savran, C. A. & Ziaie, B. Laser-treated hydrophobic paper: an inexpensive microfluidic platform. *Lab on a Chip* **11**, 1161-1165, doi:10.1039/c0lc00512f (2011).

44 Gau, H., Herminghaus, S., Lenz, P. & Lipowsky, R. Liquid morphologies on structured surfaces: From microchannels to microchips. *Science* **283**, 46-49, doi:10.1126/science.283.5398.46 (1999).

45 Varanasi, K. K., Hsu, M., Bhate, N., Yang, W. & Deng, T. Spatial control in the heterogeneous nucleation of water. *Applied Physics Letters* **95**, doi:094101 10.1063/1.3200951 (2009).

46 Chen, X. *et al.* Nanograssed Micropyramidal Architectures for Continuous Dropwise Condensation. *Advanced Functional Materials*, n/a-n/a, doi:10.1002/adfm.201101302 (2011).

47 Patankar, N. A. Supernucleating surfaces for nucleate boiling and dropwise condensation heat transfer. *Soft Matter* **6**, 1613-1620, doi:10.1039/b923967g (2010).

48 Betz, A. R., Xu, J., Qiu, H. & Attinger, D. Do surfaces with mixed hydrophilic and hydrophobic areas enhance pool boiling? *Applied Physics Letters* **97**, doi:141909 10.1063/1.3485057 (2010).

49 Betz, A. R., Jenkins, J. R., Kim, C. J., Attinger, D. & Ieee. in *2011 Ieee 24th International Conference on Micro Electro Mechanical Systems Proceedings: Ieee Micro Electro Mechanical Systems* 1193-1196 (Ieee, 2011).

50 Jo, H., Ahn, H. S., Kane, S. & Kim, M. H. A study of nucleate boiling heat transfer on hydrophilic, hydrophobic and heterogeneous wetting surfaces. *International Journal of Heat and Mass Transfer* **54**, 5643-5652, doi:10.1016/j.ijheatmasstransfer.2011.06.001 (2011).

51 Balgar, T., Franzka, S., Hasselbrink, E. & Hartmann, N. Laser-assisted fabrication of submicron-structured hydrophilic/hydrophobic templates for the directed self-assembly

of alkylsiloxane monolayers into confined domains. *Applied Physics a-Materials Science & Processing* **82**, 15-18, doi:10.1007/s00339-005-3413-z (2006).

52 Maoz, R., Cohen, S. R. & Sagiv, J. Nanoelectrochemical patterning of monolayer surfaces: Toward spatially defined self-assembly of nanostructures. *Advanced Materials* **11**, 55-61, doi:10.1002/(sici)1521-4095(199901)11:1<55::aid-adma55>3.0.co;2-8 (1999).

53 Masuda, Y., Ieda, S. & Koumoto, K. Site-selective deposition of anatase TiO2 in an aqueous solution using a seed layer. *Langmuir* **19**, 4415-4419, doi:10.1021/la020879r (2003).

54 Masuda, Y., Tomimoto, K. & Koumoto, K. Two-dimensional self-assembly of spherical particles using a liquid mold and its drying process. *Langmuir* **19**, 5179-5183, doi:10.1021/la0209435 (2003).

55 Qin, D. *et al.* Fabrication of ordered two-dimensional arrays of micro- and nanoparticles using patterned self-assembled monolayers as templates. *Advanced Materials* **11**, 1433-1437, doi:10.1002/(sici)1521-4095(199912)11:17<1433::aid-adma1433>3.0.co;2-p (1999).

56 Hohnholz, D., Okuzaki, H. & MacDiarmid, A. G. Plastic electronic devices through line patterning of conducting polymers. *Advanced Functional Materials* **15**, 51-56, doi:10.1002/adfm.200400241 (2005).

57 Li, L. *et al.* High-Performance and Stable Organic Transistors and Circuits with Patterned Polypyrrole Electrodes. *Advanced Materials* **24**, 2159-2164, doi:10.1002/adma.201104343 (2012).

58 Gillmor, S. D., Thiel, A. J., Strother, T. C., Smith, L. M. & Lagally, M. G. Hydrophilic/hydrophobic patterned surfaces as templates for DNA arrays. *Langmuir* **16**, 7223-7228, doi:10.1021/la991026a (2000).

59 Yang, J. *et al.* Rapid and reversible switching between superoleophobicity and superoleophilicity in response to counterion exchange. *Journal of Colloid and Interface Science* **366**, 191-195, doi:10.1016/j.jcis.2011.09.076 (2012).

60 Zhang, M., Zhang, T. & Cui, T. Wettability Conversion from Superoleophobic to Superhydrophilic on Titania/Single-Walled Carbon Nanotube Composite Coatings. *Langmuir* **27**, 9295-9301, doi:10.1021/la200405b (2011).

61 Zimmermann, J., Rabe, M., Artus, G. R. J. & Seeger, S. Patterned superfunctional surfaces based on a silicone nanofilament coating. *Soft Matter* **4**, 450-452, doi:10.1039/b717734h (2008).

62 Ginley, D., Green, M. A. & Collins, R. Solar energy conversion toward 1 terawatt. *Mrs Bull* **33**, 355-364 (2008).

63 Bagnall, D. M. & Boreland, M. Photovoltaic technologies. *Energ Policy* **36**, 4390-4396, doi:DOI 10.1016/j.enpol.2008.09.070 (2008).

64 Surek, T. Crystal growth and materials research in photovoltaics: progress and challenges. *J Cryst Growth* **275**, 292-304, doi:DOI 10.1016/j.jcrysgro.2004.10.093 (2005).

65 Lewis, N. S. Toward cost-effective solar energy use. *Science* **315**, 798-801, doi:DOI 10.1126/science.1137014 (2007).

66 Buonassisi, T. *et al.* Engineering metal-impurity nanodefects for low-cost solar cells. *Nat Mater* **4**, 676-679, doi:Doi 10.1038/Nmat1457 (2005).

67 Boukai, A. *et al.* Efficiency enhancement of copper contaminated radial p-n junction solar cells. *Chem Phys Lett* **501**, 153-158, doi:DOI 10.1016/j.cplett.2010.11.069 (2011).

68 De Wolf, S. *et al.* Solar cells from upgraded metallurgical grade (UMG) and plasma-purified UMG multi-crystalline silicon substrates. *Sol Energ Mat Sol C* **72**, 49-58 (2002).

69 Kwapil, W., Wagner, M., Schubert, M. C. & Warta, W. High net doping concentration responsible for critical diode breakdown behavior of upgraded metallurgical grade multicrystalline silicon solar cells. *J Appl Phys* **108**, doi:Artn 023708
Doi 10.1063/1.3463332 (2010).

70 Yoon, J. *et al.* Ultrathin silicon solar microcells for semitransparent, mechanically flexible and microconcentrator module designs. *Nat Mater* **7**, 907-915, doi:Doi 10.1038/Nmat2287 (2008).

71 Shir, D., Yoon, J., Chanda, D., Ryu, J. H. & Rogers, J. A. Performance of Ultrathin Silicon Solar Microcells with Nanostructures of Relief Formed by Soft Imprint Lithography for Broad Band Absorption Enhancement. *Nano Lett* **10**, 3041-3046, doi:Doi 10.1021/Nl101510q (2010).

72 Baca, A. J. *et al.* Compact monocrystalline silicon solar modules with high voltage outputs and mechanically flexible designs. *Energ Environ Sci* **3**, 208-211, doi:Doi 10.1039/B920862c (2010).

73 Morita, K. & Miki, T. Thermodynamics of solar-grade-silicon refining. *Intermetallics* **11**, 1111-1117, doi:Doi 10.1016/S0966-9795(03)00148-1 (2003).

74 Price, S. & Margolis, R. 2008 Solar Technologies Market Report. (U.S. Department of Energy, 2010).

75 Tian, B. Z. *et al.* Coaxial silicon nanowires as solar cells and nanoelectronic power sources. *Nature* **449**, 885-U888, doi:Doi 10.1038/Nature06181 (2007).

76 Hu, L. & Chen, G. Analysis of optical absorption in silicon nanowire Arrays for photovoltaic applications. *Nano Lett* **7**, 3249-3252, doi:Doi 10.1021/Nl071018b (2007).

77 Spinelli, P., Verschuuren, M. A. & Polman, A. Broadband omnidirectional antireflection coating based on subwavelength surface Mie resonators. *Nat Commun* **3**, 692, doi:ncomms1691 [pii]
10.1038/ncomms1691 (2012).

78 Zhu, J. *et al.* Optical absorption enhancement in amorphous silicon nanowire and nanocone arrays. *Nano Lett* **9**, 279-282, doi:10.1021/nl802886y
10.1021/nl802886y [pii] (2009).

79 Zhu, J., Hsu, C. M., Yu, Z., Fan, S. & Cui, Y. Nanodome solar cells with efficient light management and self-cleaning. *Nano Lett* **10**, 1979-1984, doi:10.1021/nl9034237 (2010).

80 Barnes, W. L., Dereux, A. & Ebbesen, T. W. Surface plasmon subwavelength optics. *Nature* **424**, 824-830, doi:Doi 10.1038/Nature01937 (2003).

81 Atwater, H. A. & Polman, A. Plasmonics for improved photovoltaic devices. *Nat Mater* **9**, 205-213, doi:Doi 10.1038/Nmat2629 (2010).

82 Shin, D. O. *et al.* A plasmonic biosensor array by block copolymer lithography. *J Mater Chem* **20**, 7241-7247, doi:Doi 10.1039/C0jm01319f (2010).

83 Ding, I.-K. *et al.* Plasmonic Dye-Sensitized Solar Cells. *Advanced Energy Materials* **1**, 52-57 (2011).

84 Zhang, J., Fu, Y., Chowdhury, M. H. & Lakowicz, J. R. Metal-enhanced single-molecule fluorescence on silver particle monomer and dimer: Coupling effect between metal particles. *Nano Lett* **7**, 2101-2107, doi:Doi 10.1021/Nl071084d (2007).

85 Hicks, E. M. *et al.* Controlling plasmon line shapes through diffractive coupling in linear arrays of cylindrical nanoparticles fabricated by electron beam lithography. *Nano Lett* **5**, 1065-1070, doi:Doi 10.1021/Nl0505492 (2005).

86 Chou, S. Y., Krauss, P. R. & Renstrom, P. J. Imprint lithography with 25-nanometer resolution. *Science* **272**, 85-87 (1996).

87 Wouters, D. & Schubert, U. S. Nanolithography and nanochemistry: Probe-related patterning techniques and chemical modification for nanometer-sized devices. *Angew Chem Int Edit* **43**, 2480-2495, doi:DOI 10.1002/anie.200300609 (2004).

88 Zschech, D. *et al.* Ordered arrays of <100>-oriented silicon nanorods by CMOS-compatible block copolymer lithography. *Nano Lett* **7**, 1516-1520, doi:10.1021/nl070275d (2007).

89 Cheng, J. Y., Mayes, A. M. & Ross, C. A. Nanostructure engineering by templated self-assembly of block copolymers. *Nat Mater* **3**, 823-828, doi:nmat1211 [pii] 10.1038/nmat1211 (2004).

90 Lee, D. H., Shin, D. O., Lee, W. J. & Kim, S. O. Hierarchically organized carbon nanotube arrays from self-assembled block copolymer nanotemplates. *Adv Mater* **20**, 2480-2485, doi:DOI 10.1002/adma.200702712 (2008).

91 Lee, D. H., Lee, W. J. & Kim, S. O. Highly Efficient Vertical Growth of Wall-Number-Selected, N-Doped Carbon Nanotube Arrays. *Nano Lett* **9**, 1427-1432, doi:Doi 10.1021/Nl803262s (2009).

92 Batchelor, G. K. *An introduction in fluid dynamics / by G. K. Batchelor*. (U.P, 1970).

93 Ishizaki, T. & Saito, N. Rapid Formation of a Superhydrophobic Surface on a Magnesium Alloy Coated with a Cerium Oxide Film by a Simple Immersion Process at Room Temperature and Its Chemical Stability. *Langmuir* **26**, 9749-9755, doi:10.1021/la100474x (2010).

94 Kwon, J. Y. *et al.* High efficiency thin upgraded metallurgical-grade silicon solar cells on flexible substrates. *Nano Lett* **12**, 5143-5147, doi:10.1021/nl3020445 (2012).

95 Zhao, J. & Green, M. A. Optimized Antireflection Coatings for High-Efficiency Silicon Solar Cells. *Ieee T Electron Dev* **38**, 1925-1934 (1991).

96 Richards, B. S. Comparison of TiO_2 and Other Dielectric Coatings for Buried-contact Solar Cells: a Review. *Prog. Photovolt: Res. Appl.* **12**, 253-281 (2004).

97 Inomata, Y., Fukui, K. & Shirasawa, K. Surface texturing of lare area multicrystalline silicon solar cells using reactive ion etching method. *Sol Energ Mat Sol C* **48**, 237-242 (1997).

98 Blakers, A. W., Wang, A., Milne, A. M., Zhao, J. & Green, M. A. 22.8% efficient silicon solar cell *Appl Phys Lett* **55**, 1363-1365 (1989).

99 Haase, C. & Stiebig, H. Thin-film silicon solar cells with efficient periodic light trapping texture. *Appl Phys Lett* **91**, doi:Artn 061116 Doi 10.1063/1.2768882 (2007).

100 Li, X. *et al.* Dual plasmonic nanostructures for high performance inverted organic solar cells. *Adv Mater* **24**, 3046-3052, doi:10.1002/adma.201200120 (2012).

101 Zschech, D. *et al.* Ordered arrays of <100>-oriented silicon nanorods by CMOS-compatible block copolymer lithography. *Nano Lett* **7**, 1516-1520, doi:10.1021/nl070275d (2007).

102 Cheng, J. Y., Mayes, A. M. & Ross, C. A. Nanostructure engineering by templated self-assembly of block copolymers. *Nat Mater* **3**, 823-828, doi:nmat1211 [pii]

10.1038/nmat1211 (2004).

103 Park, M., Harrison, C., Chaikin, P. M., Register, R. A. & Adamson, D. H. Block Copolymer Lithography: Periodic Arrays of ~1011 Holes in 1 Square Centimeter. *Science* **276**, 1401-1404 (1997).

104 Park, S. *et al.* Macroscopic 10-terabit-per-square-inch arrays from block copolymers with lateral order. *Science* **323**, 1030-1033, doi:323/5917/1030 [pii] 10.1126/science.1168108 (2009).